Journal Name

COMMUNICATION

Protic organic ionic plastic crystals based on a difunctional cation and the triflate anion: a new solid-state proton conductor

Received 00th January 20xx,
Accepted 00th January 20xx

DOI: 10.1039/x0xx00000x

www.rsc.org/

Jun Rao,[a] Vijayraghavan Ranganathan,[b] Fangfang Chen,[a] Haijin Zhu,*[a] Patrick C. Howlett,[a] Douglas R. MacFarlane[b] and Maria Forsyth*[a]

Two protic organic ionic plastic crystalline materials based on the mono- and di-protonated cations of N,N-dimethylethyldiamine, (DMEDA) and the triflate anion have been studied. The symmetrical di-protonated cation salt shows 54 °C higher melting point and 24-fold conductivity at room temperature as compared to the mono-protonated cation salt, making it a promising candidate for a solid-state proton conductor. The conductivity of this salt was further enhanced by acid doping.

Proton conducting membranes are widely used in a variety of electrochemical applications such as fuel cells and redox flow batteries.[1-3] A perfluorosulfonic polymer, such as Nafion is the most widely used proton conductor for these applications due to its high proton conductivity, excellent chemical stability and good mechanical properties.[4] However, the operating conditions of the Nafion membranes are limited to <100°C due to the presence of water being an essential condition for its high proton conductivity.[4] Thus, alternative solid-state anhydrous proton conductors are being sought for elevated temperature applications. Consequently, several studies have explored the use of ionic liquids as proton conducting electrolytes to avoid volatility, as well as obtain excellent conductivity without humidification.[5-7] These ionic liquids can be incorporated into a polymer matrix to ensure mechanical strength, but this can lead to long-term instability due to phase separation between the IL and the polymer.[1]

Organic ionic plastic crystals (OIPCs) have emerged as novel solid-state ionic conductors, with unique plastic phases that provide good mechanical flexibility and improved contact between electrodes and electrolyte.[8, 9] In addition, intrinsic ionic conductivity, non-flammability, good thermal stability and wide electrochemical windows are all desirable properties offered by OIPCs, just as with their ionic liquid analogues.[10] The development of protic organic salts as proton conductors has made important progress in recent years. Many new protic ionic liquids (PILs) and their polymer composites have been developed.[4] Similarly, OIPCs have recently been recognized as the basis for solid-state proton conductors that can exhibit excellent proton conductivity after acid doping. Rana, et al developed a new aprotic OIPC, [Choline][triflate], which can achieve good solid-phase proton conduction after triflic acid doping,[11] and good thermal stability up to 200 °C. In the temperature range of interest above 100°C, the conductivity of acid doped [Choline][triflate] can reach 2×10^{-3} S/cm at 120°C and NMR studies suggest that the proton diffusion rate is twice that of the anion.[11] Similarly, Zhu, et al have investigated the guanidinium triflate system, in which several orders of magnitude improvement in the proton conductivity can be achieved after triflic acid (HTf) doping into the GTf matrix.[12]

In the current study, we investigate the properties and the molecular dynamics of two new protic OIPCs, [DMEDAH][Tf] and $[DMEDAH_2][Tf]_2$ (Fig. 1(a,b)), based on the same parent difunctional amine, that are sufficiently conductive for solid-state proton conductor applications in the sub 100°C region. Upon acid doping, the conductivity of $[DMEDAH_2][Tf]_2$ reaches $10^{-3.5}$ S/cm at 50°C.

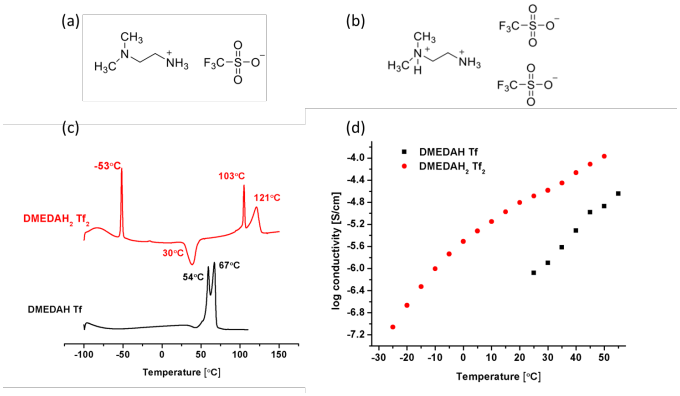

Fig. 1 Structural formulas of [DMEDAH][Tf] (a) and $[DMEDAH_2][Tf]_2$ (b); DSC traces (c) and ionic conductivity (d) of neat [DMEDAH][Tf] and $[DMEDAH_2][Tf]_2$.

Both samples were synthesized via the neutralization reaction of N,N-dimethylethylenediamine and triflic acid at the corresponding stoichiometric ratios. Detailed synthetic procedures are described in the supporting information. The

[a] ARC Centre of Excellence for Electromaterials Science (ACES), Institute for Frontier Materials (IFM), Deakin Univeristy, Melbourne Campus at Burwood, Burwood VIC 3125, Australia.
[b] ARC Centre of Excellence for Electromaterials Science (ACES), Department of Materials Engineering, Monash University, Wellington Rd, Clayton, VIC 3800, Australia

Electronic Supplementary Information (ESI) available: Synthesis, Experimental, NMR, DFT calculation. See DOI: 10.1039/x0xx00000x

Differential Scanning Calorimetric (DSC) traces (Fig. 1(c)) of the neat [DMEDAH][Tf] and [$DMEDAH_2$][$Tf]_2$ show that these materials pass through one or two solid-solid phase transitions (a common property of plastic crystals) prior to melting, which suggests that the structure of samples changes with increasing temperature. Although the chemical structures of both samples are quite similar, their thermal properties are completely different. For [DEMDAH][Tf], a solid-solid transition at 54°C is observed which is close to the melting peak temperature of 67°C. For [$DMEDAH_2$][$Tf]_2$, two solid-solid transitions are observed, with the first transition at -53°C, and the second transition at 103°C, which is close to its melting point of 121°C. Interestingly, while both the solid-solid transitions exhibit a sharp DSC feature, the melting peak of the [$DMEDAH_2$][$Tf]_2$ is rather broad. This behaviour has been observed in similar OIPC systems,[13-15] and confirmed by solid-state NMR lineshape analysis and in-situ NMR imaging techniques. This broad melting behaviour, inherent in many of the OIPCs, indicates partial liquefaction over a large temperature range, thereby leading to a substantial increase in conductivity while maintaining the mechanical properties and flexibility of the solid. In addition to the endothermic peaks, a broad exothermic (cold recrystallization) peak (~30°C) due to supercooling is observed in the heating trace. The melting point of [$DMEDAH_2$][$Tf]_2$ is approximately 50°C higher than that of [DMEDAH][Tf], which may be due to the stronger interactions between the doubly charged cation and the anions. In supporting information, the experimental together with simulated ^{13}C CPMAS NMR shifts suggest that the cation structure is more symmetric in [$DMEDAH_2$][$Tf]_2$, which can explain the higher melting point of [$DMEDAH_2$][$Tf]_2$ according to the literature. [16]

The conductivity results in Fig. 1(d) show that [$DMEDAH_2$][$Tf]_2$ has more than one order of magnitude higher ionic conductivity than [DMEDAH][Tf] in the temperature range from 25°C to 50°C. In particular, at 25 °C, the ionic conductivity of [$DMEDAH_2$][$Tf]_2$ shows a 24-fold increase compared to [DMEDAH][Tf] ($10^{-6.1}$ S/cm), reaching $10^{-4.6}$ S/cm. This is an extremely high solid-state proton conductivity (without presence of a liquid phase), the highest to date to the best of our knowledge. One explanation for the higher conductivity of [$DMEDAH_2$][$Tf]_2$ is that the second proton attached to the cation is more dissociable compared to the first proton, thus it can more easily transport. This is evidenced in general in the aqueous pK_a values for this type of diamino molecule, where the pK_{a1} and pK_{a2} values are typically 2 -3 units apart.[17]

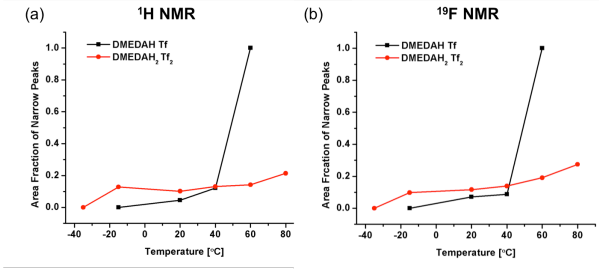

Fig. 2 The area fraction of narrow component of NMR peaks at different temperatures in neat [DMEDAH][Tf] and [$DMEDAH_2$][$Tf]_2$ for the cation (^{1}H) and anion (^{19}F) species.

Solid-state NMR provides us with a versatile tool to study the structure and dynamics of materials at the molecular level.[18-20] In the present samples, ^{1}H and ^{19}F nuclei only exist in the cation and anion respectively, thus the NMR spectra allow us to probe the local dynamics of the individual ion species. The static ^{1}H and ^{19}F NMR spectra of both samples exhibit a typical feature of a narrow line superimposing on a broad line (see Fig. (S3)). Based on this model, the spectra thus can be roughly deconvoluted into two components, where the narrow line represents the mobile component and the broad line represents the immobile component.[21, 22] Fig. 2 compares the area fraction of the narrow component of the ^{1}H and ^{19}F NMR spectra peaks for the pure [DMEDAH][Tf] and [$DMEDAH_2$][$Tf]_2$ measured at different temperature. Below 40°C, the fraction of narrow peaks in [$DMEDAH_2$][$Tf]_2$ is higher than that of [DMEDAH][Tf], which can explain the higher ionic conductivity of the former. When the temperature approaches 60°C, the narrow peaks in the [DMEDAH][Tf] spectra increase sharply to 100 %, suggesting a dramatic growth in the proportion of mobile cations, corresponding to the solid-solid transition before the melting point. A similar result has been observed for other plastic crystal materials such as pyrrolidinium tetrafluoroborate,[20] and phosphonium hexafuorophosphate,[13] where in plastic crystal phase I (the highest temperature solid phase), fast isotropic molecular motion sets in and both the cation and anion (^{1}H and ^{19}F) NMR spectra exhibit an extremely narrowed lineshape. The ^{19}F narrow component fraction shows a similar trend to that observed in the ^{1}H spectra, suggesting coupled molecular dynamics between the cations and anions.

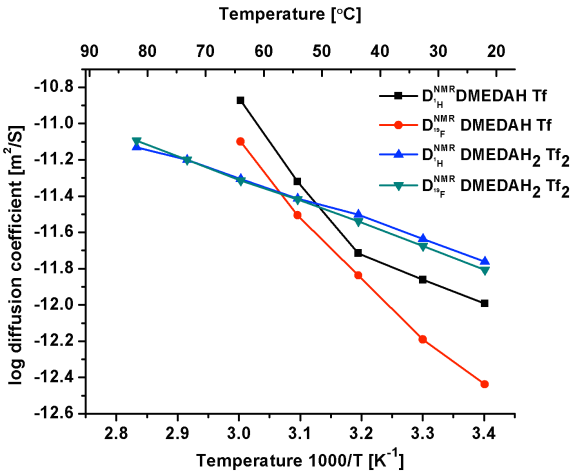

Fig. 3 Diffusion coefficient at different temperatures measured by NMR.

The static solid-state ^{1}H and ^{19}F NMR results show the existence of mobile species in both samples below their respective melting points, as suggested by the presence of extremely narrow lines. To probe the translational motion and measure the diffusion coefficients of various species in the solids, pulse-field gradient (PFG) NMR experiments were performed. Fig. 3 presents diffusion data for both cation and anion in [DMEDAH][Tf] and [$DMEDAH_2$][$Tf]_2$. At 40 °C and below, both the cation and anion of [DMEDAH][Tf] show lower diffusion coefficients, as compared to [$DMEDAH_2$][$Tf]_2$, despite the higher melting point of the latter compound. The lower diffusivity, in combination with the smaller percentage of the

diffusive species as suggested in Figure 2, explains the lower conductivity of [DMEDAH][Tf] at lower temperatures. The diffusivity of the cation and anion are similar in $[DMEDAH_2][Tf]_2$, while in the [DMEDAH][Tf] sample the cation diffusivity is higher than that of the anion. This suggests that the cation and anion species in $[DMEDAH_2][Tf]_2$ are more strongly correlated than in DMEDAH Tf, which can be explained by the stronger hydrogen bonding in the former compound. This is also supported by the DSC results which show an approximately 50 °C increase in the melting point compared to [DMEDAH][Tf].

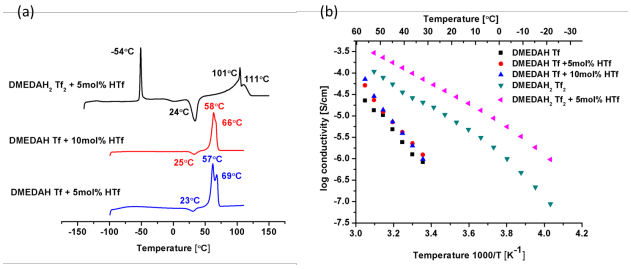

Fig. 4 DSC traces (a) and ionic conductivity at different temperatures (b) of acid doped [DMEDAH][Tf] and $[DMEDAH_2][Tf]_2$.

From previous studies,[12, 23] some plastic crystals display orders of magnitude higher conductivity after acid doping, which provides a useful approach to improve the conductivity. Thus, we have also investigated the feasibility of acid addition in both protic organic salts studied here to further enhance the proton conductivity. The DSC traces for the triflic acid doped sample in Fig.4 (a) show only minor changes, compared to the neat samples, Fig. 1(c). For [DEMDAH][Tf], after 5mol% and 10mol% triflic acid doping the solid-solid transition and melting point are still 57°C and 68°C respectively. An exothermic peak can be identified at 25°C in the heating scan for both doped samples, which is a recrystallization process related to supercooling of the samples. Two solid-solid transitions at -54°C and 101°C are observed for 5mol% HTf doped $[DMEDAH_2][Tf]_2$ with recrystallization and melting peaks at 24°C and 111°C respectively.

The conductivity data in Fig.4 (b) show that the doped [DMEDAH][Tf] samples have similar conductivity; this can be expected since the additional proton will primarily be transferred to the available amino group of the cation, thus the number of mobile protons does not increase substantially. On the other hand, upon addition of 5 mol% acid to $[DMEDAH_2][Tf]_2$, the conductivity increased significantly, reaching $10^{-3.6}$ S/cm at 50 °C. This conductivity enhancement can be understood in terms of the increased number of charge carriers (dissociable protons from the doped acid) and the existing percolated conducting pathways in the $[DMEDAH_2][Tf]_2$ system.

In summary, this communication describes the properties of two protic organic salts [DMEDAH][Tf] and $[DMEDAH_2][Tf]_2$. $[DMEDAH_2][Tf]_2$ has a symmetrical cation structure, and exhibits the higher melting point of the two. Remarkably, despite the significantly higher melting point, the $[DMEDAH_2][Tf]_2$ sample exhibits 24-fold enhancement in conductivity as compared to the [DMEDAH][Tf] sample. PFG-NMR results show that the cation and anion in $[DMEDAH_2][Tf]_2$ exhibit a strongly coupled translational motion. This coupled motion, however, is not observed in the [DMEDAH][Tf] sample. Upon addition of 5mol% acid to $[DMEDAH_2][Tf]_2$, the conductivity increases significantly, reaching $10^{-3.6}$ S/cm at 50 °C. This new family of difunctional ammonium based plastic crystals developed in this work exhibits an exciting solid-state conductivity and thus can be a promising candidate for a solid-state proton conductor in fuel cells, redox flow batteries, and many other electrochemical devices.

The authors are grateful to the Australian Research Council for funding through the ARC Centre of Excellence for Electromaterials Science. MF and DRM acknowledge the ARC for funding under the Laureate Fellowship program. The ARC is also acknowledged for funding Deakin University Magnetic Resonance Facility through LIEF grant LE110100141.

Notes and references

1. S. J. Peighambardoust, S. Rowshanzamir and M. Amjadi, *International Journal of Hydrogen Energy*, 2010, **35**, 9349-9384.
2. X. Li, H. Zhang, Z. Mai, H. Zhang and I. Vankelecom, *Energy & Environmental Science*, 2011, **4**, 1147.
3. B. Kumar, M. Llorente, J. Froehlich, T. Dang, A. Sathrum and C. P. Kubiak, *Annual review of physical chemistry*, 2012, **63**, 541-569.
4. U. A. Rana, M. Forsyth, D. R. MacFarlane and J. M. Pringle, *Electrochimica Acta*, 2012, **84**, 213-222.
5. N. Akihiro, B. H. S. Md. Abu, K. Kenji, M. Shigenori, H. Kikuko and W. Masayoshi, *J. Phys. Chem. B*, 2003, **107**, 4024-4033.
6. H. Nakamoto, A. Noda, K. Hayamizu, S. Hayashi, H.-o. Hamaguchi and M. Watanabe, *The Journal of Physical Chemistry C*, 2007, **111**, 1541-1548.
7. M. Martinez, Y. Molmeret, L. Cointeaux, C. Iojoiu, J.-C. Leprêtre, N. El Kissi, P. Judeinstein and J.-Y. Sanchez, *Journal of Power Sources*, 2010, **195**, 5829-5839.
8. D. R. MacFarlane and M. Forsyth, *Advanced materials*, 2001, **13**, 957-966.
9. J. M. Pringle, *Physical Chemistry Chemical Physics*, 2013, **15**, 1339-1351.
10. D. R. MacFarlane, N. Tachikawa, M. Forsyth, J. M. Pringle, P. C. Howlett, G. D. Elliott, J. H. Davis, M. Watanabe, P. Simon and C. A. Angell, *Energy Environ. Sci.*, 2014, **7**, 232-250.
11. U. A. Rana, R. Vijayaraghavan, D. R. MacFarlane and M. Forsyth, *Chemical Communications*, 2011, **47**, 6401-6403.
12. H. Zhu, U. a. Rana, V. Ranganathan, L. Jin, L. A. O'Dell, D. R. MacFarlane and M. Forsyth, *J. Mater. Chem. A*, 2014, **2**, 681-691.
13. L. Jin, K. M. Nairn, C. M. Forsyth, A. J. Seeber, D. R. MacFarlane, P. C. Howlett, M. Forsyth and J. M. Pringle, *Journal of the American Chemical Society*, 2012, **134**, 9688-9697.
14. K. Romanenko, L. Jin, P. Howlett and M. Forsyth, *Chemistry of Materials*, 2016, **28**, 2844-2851.
15. X. Chen, H. Tang, T. Putzeys, J. Sniekers, M. Wubbenhorst, K. Binnemans, J. Fransaer, D. E. De Vos, Q. Li and J. Luo, *Journal of Materials Chemistry A*, 2016.
16. W. Zheng, A. Mohammed, L. G. Hines Jr, D. Xiao, O. J. Martinez, R. A. Bartsch, S. L. Simon, O. Russina, A. Triolo and E. L. Quitevis, *The Journal of Physical Chemistry B*, 2011, **115**, 6572-6584.

17. S. Lalwani, E. Tutu and G. Vigh, *Electrophoresis*, 2005, **26**, 2503-2510.
18. H. Zhu, D. MacFarlane and M. Forsyth, *The Journal of Physical Chemistry C*, 2014, **118**, 28520-28526.
19. A. H. Shah, J. Li, H. Yang, U. A. Rana, V. Ranganathan, H. M. Siddigi, D. R. MacFarlane, M. Forsyth and H. Zhu, *Journal of Materials Chemistry A*, 2016, **4**, 7615-7623.
20. H. Zhu, F. Chen, L. Jin, L. A. O'Dell and M. Forsyth, *ChemPhysChem*, 2014, **15**, 3720-3724.
21. H. Zhu, H. P. Huinink, O. C. Adan and K. Kopinga, *Macromolecules*, 2013, **46**, 6124-6131.
22. H. Zhu, H. P. Huinink, P. C. Magusin, O. C. Adan and K. Kopinga, *Journal of Magnetic Resonance*, 2013, **235**, 109-114.
23. U. A. Rana, R. Vijayaraghavan, D. R. MacFarlane and M. Forsyth, *Journal of Materials Chemistry*, 2012, **22**, 2965-2974.

